ISSN 1330-3651 (Print), ISSN 1848-6339 (Online)
https://doi.org/10.17559/TV-20220505073935
Original scientific paper

A Simplified Method for Analyzing Overall Stability of Flexural-Type Braced Frame Structures

Shuwei LAN, Chi XIAO*, Xu CHEN, Chunhua WANG

Abstract: It is difficult to determine the effective length coefficient of weakly braced frame columns using the effective length coefficient method. When the stability of braced frame structures is calculated using the effective length coefficient method, it cannot reflect the effect of the brace on the frame, the mutual support of columns on the same floor, and vertical interactions between different floors, which is easy to lead to unreasonable design. In this study, based on a spring-rocking column model, the structural transformation concept was used to transform the second-order problem of determining the critical force of braced frame structures into a first-order problem of calculating the lateral stiffness of the structure. First, the repetitive frame element was used to obtain the lateral stiffness of each floor, and the second-order effect coefficient was used to determine the load stiffness of the floor. Next, the lateral stiffness and load stiffness of each floor was assembled. Finally, the principle in which the load stiffness reduces the lateral stiffness of the structure to zero when the braced frame structure buckles laterally were applied to derive a formula to directly calculate the critical force of the flexural-type brace frame structure. This formula reflects the interactions between the braced structure and the frame, the mutual support of columns on the same floor, and the vertical interactions between different floors. Therefore, it can compensate for the deficiency in which the criterion cannot calculate the critical force of braced frame structures and is suitable for quantitatively analyzing the vertical interactions between different floors of braced frame structures.

Keywords: critical factor; critical force; flexural-type braced structures; frame; lateral stiffness; load stiffness

1 INTRODUCTION

Braced frame structures are widely used in various engineering applications. Finite element software is mainly used to directly calculate the critical force of braced frame structures. Because finite element software is being increasingly used to compute the stability of structures, how to check finite element results is an unavoidable problem. Calculation tables of the effective length coefficient for nonlateral and free lateral displacement frame columns have been provided by major national organizations [1-3]. Generally, formulae and tables for analyzing weakly braced frame structures are lacking because the bracing stiffness of braced frame structures cannot satisfy the requirement for strong bracing stiffness of nonlateral displacement frame structures. If the critical force of weakly braced frame structures is solved based on the effective length coefficient of nonlateral displacement frame columns, the structure will be unsafe. If it is solved based on the free lateral displacement frame columns, the results will be conservative. To solve these problems, some researchers conducted studies [4-14]. Among them, Chen [6] and Mageirou [7], investigated the stability of braced frame columns and derived formulas to compute the effective length coefficient of frame columns with arbitrary bracing stiffness through computer calculations. Rosman [8] and Bozdogan [9] analyzed overall stability of frame-shear wall structures. The frame was continuously transformed into a shear cantilever beam and shear wall to form a double-lateral force resistance system. The finite integral method is used to determine the critical force through computer calculations, which is inconvenient for practical applications. Tong [14] derived the critical force of a flexural-type braced frame. Based on numerous finite element calculations, empirical formulas for determining the critical force have been summarized. The solution accuracy of this method is influenced by the load type and the finite element analysis method.

In this study, the structural transformation method was used to obtain the critical force of flexural-type braced frame structures by transforming the second-order problem into a first-order problem. The lateral stiffness of structures was determined by analyzing the calculation model of the separation column of braced frame structures. The method for calculating the critical force of a single-braced column was extended to the entire structure to determine the critical force of flexural-type braced frame structures.

2 CALCULATION MODEL OF SEPARATION COLUMN OF FLEXURAL-TYPE BRACED FRAME STRUCTURES

With an increase in the height of the building and a decrease in braced stiffness, flexural characteristics are dominant, and the shear deformation effect can be ignored. Braced structures can be either a shear wall or steel braces. Flexural-type braced frame structures are shown in Fig. 1.

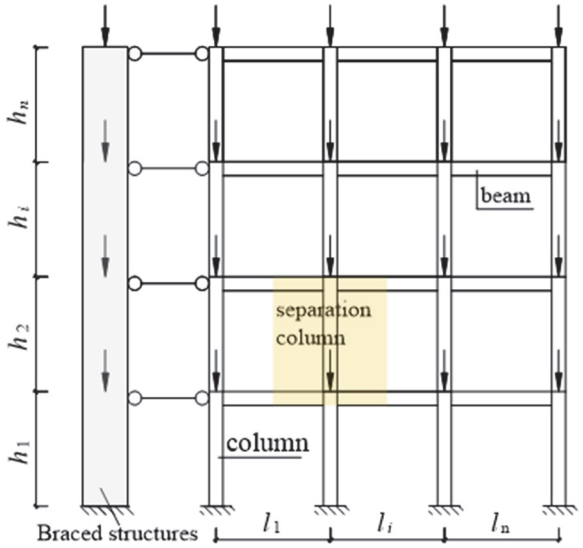

Figure 1 Flexural-type braced frame structures

The frame and bracing structure are connected by the rigid-connecting rod reflecting the floor effect. The vertical load on each floor is simplified as concentrated loads on

the top of each column and shear wall. The stability problem of flexural-type braced frame structures is more complicated than that of pure frame structures because of the existence of the flexural-type brace, and a direct solution of the overall stability of the entire structure becomes complex. Therefore, it is necessary to develop a simple and practical method for calculating the critical force of flexural-type braced frame structures.

2.1 Calculation Model of Spring-rocking Column

The separation column method [15] was adopted to separate the local column from flexural-type braced frame structures. Three springs can be used to simulate the column end constraints of each separated column of the flexural-type braced frame structures, as shown in Fig. 2. The horizontal spring with lateral displacement stiffness c_w acts on the top of the separation column, which is equivalent to the lateral bracing effect of the braced structure acting on the frame columns. This approach can accurately reflect the interaction between the braced structure and frame columns. The top and bottom of the separation column are subjected to rotational constraints, and their rotational stiffness parameters are c_1 and c_2, respectively.

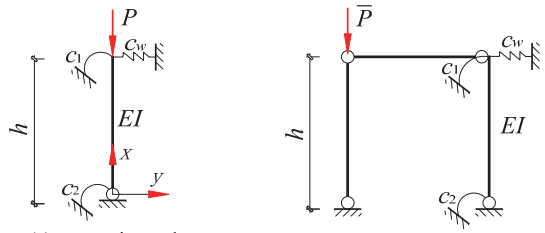

(a) separation column (the original structure)

(b) The extended structure

Figure 2 Calculation diagram of separation column

$R_1 = c_1 / 6i_c$, $R_2 = c_2 / 6i_c$, and $\bar{c}_w = c_w h^2 / i_c$ are defined. i_c is the linear stiffness of the separation column, and $\bar{c}_w$ is the relative stiffness of the bracing spring. As shown in Fig. 2a, the stability characteristic equation of the three-spring separation column is expressed as follows [16]:

$$\begin{aligned} &36\bar{c}_w R_1 R_2 \left(2-2\cos\varepsilon-\varepsilon\sin\varepsilon\right)+6\bar{c}_w\left(R_1+R_2\right)\cdot \\ &\cdot\varepsilon\left(\sin\varepsilon-\varepsilon\cos\varepsilon\right)+\left(\bar{c}_w+36R_1R_2\right)\varepsilon^3\sin\varepsilon+ \\ &+6\left(R_1+R_2\right)\varepsilon^4\cos\varepsilon-\varepsilon^5\sin\varepsilon=0 \end{aligned} \tag{1}$$

where $\varepsilon = h\sqrt{P/EI}$ is the dimensionless characteristic coefficient of the column.

The stable characteristic equation is a multivariable transcendental equation. Because it is challenging to solve it directly, there is an urgent need to develop a convenient method for the application. Because the rocking column cannot provide stiffness, only when it is attached to a stable structure, the attached structure can provide stiffness to maintain the rocking column stability and resist loads. This behavior of the rocking column was considered in establishing the extended structure of the separation column, as shown in Fig. 2b. Because the extended structural load only acts on the rocking column, the critical state equation of the extended structure is an algebraic equation, which is convenient to solve. Because the rocking column cannot provide stiffness, the lateral stiffness values of the original and expanded structures are equal. Moreover, the extended structure can be simplified into a spring-rocking column model [17], as shown in Fig. 3.

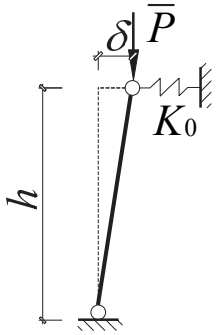

Figure 3 Spring - rocking column model

In the spring-swing column model, the spring stiffness K_0 is the lateral stiffness of the original structure. $\overline{P}$ is applied to the top of the rocking column to induce lateral displacement δ, and the moment $\overline{P}\delta - K_0\delta\cdot h = 0$ is applied to the bottom of the spring-rocking column model. The critical balance equation of the spring-rocking column model is expressed as follows:

$$K_0 - \frac{\overline{P}_{\mathrm{cr}}}{h} = 0 \tag{2}$$

The physical interpretation of Eq. (2) is the degree to which spring stiffness is weakened by an external load. When the spring-rocking column is in a critical state, the spring stiffness decreases to zero and the column becomes unstable. The critical force of the extended structure is defined as $\overline{P}_{\mathrm{cr}} = \frac{\overline{P}_{\mathrm{cr}}}{P_{\mathrm{cr}}}\frac{P_{\mathrm{cr}}}{P}P = \alpha\lambda P$, where P_{cr} is total critical force of the original structure, and P is total load of the original structure. The critical balance Eq. (2) can be transformed into Eq. (3).

$$K_0 - \alpha\lambda\frac{P}{h} = 0 \tag{3}$$

where α is the second-order effect factor, and its calculated value is equal to $\overline{P}_{\mathrm{cr}} / P_{\mathrm{cr}}$; the ratio, P/h, has the same unit with the lateral stiffness and is related to load P. It is the load stiffness and is denoted K_p. λ is the critical factor, and its calculated value equals P_{cr}/P. When the structure is in a critical state, the critical factor is equal to 1.0.

2.2 Second-Order Effect Factor of Separation Column

As shown in Fig. 2b, load $\overline{P}$ is applied to the top of the rocking column, and the top of the column generates lateral displacement δ. This load is equivalent to an imaginary horizontal force $T = \overline{P}\delta / h$ on the top of the column, as shown in Fig. 4.

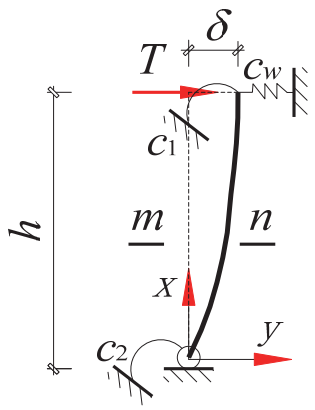

Figure 4 Calculation diagram of extended structure of separation column

Based on the balance condition of the force, Eq. (4) can be derived.

$$\sum F_X = 0, f_{AX} = 0; \quad \sum F_Y = 0, f_{Ay} = c_w\delta - T \tag{4}$$

The column was cut off from Section *m-n*, and the lower section was selected as the research object. The bending moment of the *m-n* section was balanced as follows:

$$f_{Ax}y - f_{Ay}x - M_{mn} - c_2 y_0' = 0 \tag{5}$$

where $M_{\text{mn}} = -EIy''$.

The equilibrium differential equation can be derived from Eqs. (4) and (5):

$$EIy'' - \left(c_w - \overline{P}/h\right)\delta x - c_2 y_0' = 0 \tag{6}$$

The general solution to Eq. (6) is expressed as follows:

$$y = \frac{c_w - \overline{P}/h}{6EI}\delta x^3 + \frac{c_2 y_0'}{2EI}x^2 + Ax + B \tag{7}$$

The following boundary conditions exist: $x = 0, y = 0$, $x = h$, $EIy'' + c_1 y' = 0, y = \delta$. By substituting the above boundary conditions into Eq. (7), the critical force of the separated column of the extended structure can be calculated using Eq. (8).

$$\overline{P}_{\text{cr}} = \frac{EI}{h^2}\left(\frac{6(R_1+R_2)+36R_1R_2}{1+2(R_1+R_2)+3R_1R_2} + \bar{c}_w\right) \tag{8}$$

Because an equal relationship exists between the lateral stiffness of the extended structure of the separation column and the lateral stiffness of the original structure, lateral stiffness k_{ij} of the separation column at the j^{th} column ($1 \le j \le m$) on the i^{th} floor ($1 \le i \le n$) of flexural-type braced frame structures under no axial pressure can be determined from Eq. (8).

$$k_{ij} = \frac{\overline{P}_{\text{cr}}}{h} = \frac{EI}{h^3}\left(\frac{6(R_1+R_2)+36R_1R_2}{1+2(R_1+R_2)+3R_1R_2} + \bar{c}_w\right) \tag{9}$$

In Eq. (9), R_1 and R_2 are the ratios of the sum of the linear stiffness of the upper and lower beams of the column, respectively, to the linear stiffness of the column.

In practice, relative stiffness $\bar{c}_w$ of the bracing spring provided by flexural-type braced frame structures cannot be infinite. When the linear stiffness ratios, R_1 and R_2, are provided, the critical force of the column gradually increases as $\bar{c}_w$ increases from zero. When $\bar{c}_w$ reaches a constant value, the column buckling is controlled by nonlateral instability. Theoretically, the increase in $\bar{c}_w$ at this time cannot increase the critical load. This fixed value is called the lateral critical stiffness and is denoted $\bar{c}_{wT}$, which can be obtained from Eq. (10) [14].

$$\begin{aligned}\bar{c}_{wT} = {} & [\varepsilon_1^5 \sin\varepsilon_1 - 6(R_1+R_2)\varepsilon_1^4\cos\varepsilon_1 - 36R_1 \cdot \\ & \cdot R_2\varepsilon_1^3\sin\varepsilon_1]/[\varepsilon_1^3\sin\varepsilon_1 + 36R_1R_2(2-2\cos\varepsilon_1 - \\ & -\varepsilon_1\sin\varepsilon_1) + 6(R_1+R_2)\varepsilon_1(\sin\varepsilon_1 - \varepsilon_1\cos\varepsilon_1)]\end{aligned} \tag{10}$$

where ε_1 is the dimensionless eigenvalues of nonlateral displacement frame columns, defined as follows:

$$\varepsilon_1 = \pi\frac{3+2(R_1+R_2)+1.28R_1R_2}{3+1.4(R_1+R_2)+0.64R_1R_2} \tag{11}$$

When the relative stiffness, $\bar{c}_w$, of the elastic horizontal constraint spring ranges between zero and critical stiffness $\bar{c}_{wT}$, it is a weakly braced elastic lateral displacement column, and the critical load of the column ranges between the lateral displacement column ($\bar{c}_w = 0$) and the nonlateral displacement column ($\bar{c}_w = \bar{c}_{wT}$). When R_1 and R_2 do not significantly differ, a linear relationship exists between the critical load of the elastic lateral displacement column and the relative stiffness, $\bar{c}_w$, of the bracing spring. After function fitting of the solution results, the approximate calculation equation for the critical load of the elastic lateral displacement columns can be derived as follows.

$$\begin{aligned}P_{\text{cr}} = {} & [\left(1 - \frac{\bar{c}_w}{\bar{c}_{wT}}\right)\frac{R_1+R_2+7.5R_1R_2}{1.52+4(R_1+R_2)+7.5R_1R_2} + \\ & + \left(\frac{3+2(R_1+R_2)+1.28R_1R_2}{3+1.4(R_1+R_2)+0.64R_1R_2}\right)^2 \cdot \frac{\bar{c}_w}{\bar{c}_{wT}}] \cdot \frac{\pi^2 EI}{h^2}\end{aligned} \tag{12}$$

From Eqs. (8) and (12), the second-order effect factor of an arbitrary separation column of a flexural-type braced frame structure can be derived as follows.

$$\begin{aligned}\alpha_{ij} = \frac{\overline{P}_{\text{cr}}}{P_{\text{cr}}} = {} & \frac{1}{\pi^2} \times \left(\frac{6(R_1+R_2)+36R_1R_2}{1+2(R_1+R_2)+3R_1R_2} + \bar{c}_w\right) / \\ & /[(1 - \frac{\bar{c}_w}{\bar{c}_{wT}})\frac{R_1+R_2+7.5R_1R_2}{1.52+4(R_1+R_2)+7.5R_1R_2} + \\ & + \left(\frac{3+2(R_1+R_2)+1.28R_1R_2}{3+1.4(R_1+R_2)+0.64R_1R_2}\right)^2 \cdot \frac{\bar{c}_w}{\bar{c}_{wT}}]\end{aligned} \tag{13}$$

When the lateral bracing spring stiffness $c_w \geq c_{wT}$ is provided by the braced structures, the critical force of the column cannot be increased further by increasing the bracing stiffness. When $\frac{\bar{c}_w}{c_{wT}} = 1$ is adopted, the second-order effect factor of the separation column is obtained using Eq. (14).

$$\alpha_{ij} = \frac{1}{\pi^2} \times \left(\frac{6(R_1+R_2)+36R_1R_2}{1+2(R_1+R_2)+3R_1R_2} + \bar{c}_w \right) \cdot \cdot \left(\frac{3+1.4(R_1+R_2)+0.64R_1R_2}{3+2(R_1+R_2)+1.28R_1R_2} \right)^2 \quad (14)$$

On the floor where the flexural-type braced frame structure $c_{wi} \geq c_{wTi}$ is located, the lateral bracing stiffness of the floor can be evenly distributed to each column, and the second-order effect factor of the column can be calculated using Eq. (14). This type of floor is typically the first or second floor of a building. The critical lateral stiffness c_{wTi} of the floor is calculated using Eq. (15).

$$c_{wTi} = \sum_{j=1}^{m} \bar{c}_{wTij} \cdot EI_{cij} / h_i^3 \quad (15)$$

where $\bar{c}_{wTij}$ is the critical lateral stiffness of the j^{th} column on the i^{th} floor, which can be determined using Eq. (10). EI_{cij} is the bending stiffness of the j^{th} column on the i^{th} floor, and m is the total number of frame columns of the flexural-type braced frame structure.

When the lateral bracing spring stiffness, $\bar{c}_w$, provided by the bracing structure is between zero and $\bar{c}_{wT}$, the difference between R_1 and R_2 is small (less than 20 times), the relative stiffness $\bar{c}_w$ changes from zero to $\bar{c}_{wT}$, and the change in the value calculated using Eq. (14) is within 4%. Therefore, the second-order effect factor of the corresponding separation column can be used for the approximate calculation, as $\bar{c}_w = 0$.

$$\alpha_{ij} = \frac{6}{\pi^2} \frac{R_1+R_2+6R_1R_2}{1+2(R_1+R_2)+3R_1R_2} \cdot \cdot \frac{1.52+4(R_1+R_2)+7.5R_1R_2}{R_1+R_2+7.5R_1R_2} \quad (16)$$

After the second-order effect factor α_{ij} and lateral stiffness k_{ij} of any separation column of the flexural-type braced frame structures are obtained, the critical force of any single separation column can be determined using Eq. (3). Although the interaction between the braced structures and frame columns can be considered, it is impossible to reflect the mutual support of columns on the same floor and the vertical interaction between different floors for flexural-type braced frame structures. Ignoring both mutual support effects usually induces a significant error between the critical force calculated using the proposed method and the exact solution.

Therefore, the aim of this study is to extend the method for determining the critical force of a single separation column to the analysis solution of the overall stability of flexural-type braced frame structures. In addition, we attempted to transform the second-order problem of obtaining the critical force into a first-order problem of determining the lateral stiffness of flexural-type braced frame structures based on the second-order effect factor.

3 OVERALL LATERAL STIFFNESS OF FLEXURAL-TYPE BRACED FRAME STRUCTURES

When analyzing the overall stability of a flexural-type braced frame structure under a vertical load, the continuous flexural-type braced structure is discretized based on the action of rigid floors. This is equivalent to applying a horizontal elastic support at the floor of the frame, as shown in Fig. 5a.

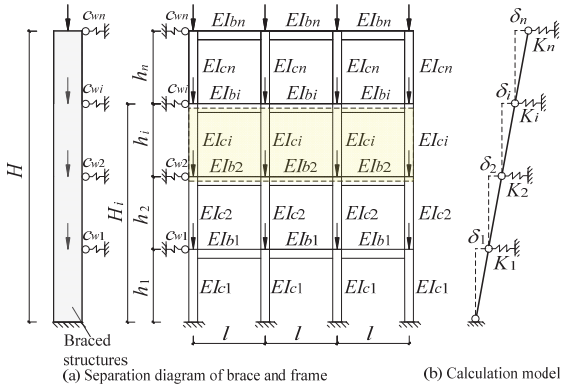

Figure 5 Calculation model of flexural-type braced frame structure

It is assumed that the relative displacement δ_i between floors is generated under the vertical load on the i^{th} floor in obtaining the lateral stiffness of each floor of the flexural-type braced frame structures. The lateral stiffness of the i^{th} floor is denoted k_i. The simplified model is shown in Fig. 5b. The lateral stiffness of each floor is regarded as a spring, and the overall lateral stiffness of the flexural-typed braced frame structure can be adopted as a series connection of each spring. Therefore, the relationship between the overall lateral stiffness, K_i, of each floor of the flexural-type braced frame structure and the lateral stiffness of each floor is expressed as follows:

$$\frac{1}{K_i} = \frac{1}{k_1} + \frac{1}{k_2} + \ldots + \frac{1}{k_i} \quad (17)$$

where K_i is the overall lateral stiffness of the i^{th} floor ($1 \leq i \leq n$), $k_1, k_2, \cdots, k_i$ are the lateral stiffness parameters for each floor, which is the superposition of the lateral stiffness of the frame on the floor and the lateral stiffness of the flexural-type brace.

3.1 Story Repetitive Element of Frame

When the overall lateral stiffness of a flexural-type braced frame structure is solved directly using Eq. (17), it is necessary to calculate the lateral stiffness of columns sequentially and assemble them to obtain the lateral stiffness of each floor. Generally, many members exist in flexural-type braced frame structures, and the solution

process is complex. Therefore, there is an urgent need to develop convenient calculation methods.

Fig. 5a shows the frame structure element, it is the filling diagram of the i^{th} floor of the flexural-type braced frame structures. The frame structure element comprises beam elements and column elements rigidly connected. The beam element is a part of the adjacent floor. The same section of beams and columns is repeatedly arranged on many floors; therefore, the structural element of this schematic is called a story repetitive element. Half of the corresponding eigenvalue of the beam section was adopted for the beam element in the repetitive floor element. It was assumed that the antibending point of the beam was located at the midspan, and the inflection point of the column was located at half of the story height, ignoring the axial force effect of the member. The deformation and boundary conditions of the story repetitive element of the story repetitive elements of the frame are shown in Fig. 6.

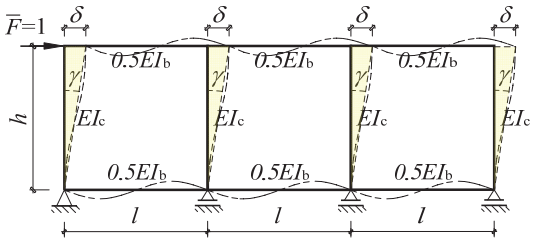

Figure 6 Deformation and boundary conditions of story repetitive element

If the floor lateral stiffness of the frame is to be determined, the story repetitive element should be analyzed to prevent tedious calculations of the floor stiffness by computing the lateral stiffness of the frame column assembly. However, the multispan frame repetitive element is a high-order statically indeterminate problem; hence, it is difficult to directly obtain the exact solution of its floor lateral stiffness k. Therefore, it is appropriately simplified based on the assumption that each column on the same floor produces the same lateral displacement δ. Because the shear force of the floor is distributed according to the lateral stiffness of the column, the column end constraint of the side column of the story repetitive element is weaker than that of the middle column, and the ratio of the D-value of the lateral stiffness of both columns is approximately 1/2. Therefore, it can be assumed that the shear distributed by the side column is half that of the middle column. The horizontal force, $\overline{F}$, was applied to the top of the story repetitive element (Fig. 6). Based on the above assumptions, it is easy to plot the bending moment diagram of the half-symmetrical story repetitive element, as shown in Fig. 7 (where m is the total number of columns of the story repetitive element).

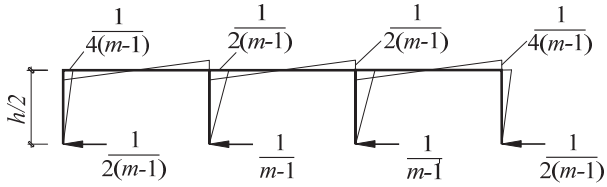

Figure 7 Bending moment diagram of half-symmetry story repetitive element

Figure multiplication [18] can be applied to obtain the floor relative displacement, δ, of the story repetitive element.

$$\delta = \frac{(2m-3)h^3}{24EI_c(m-1)^2} + \frac{h^2 l}{12EI_b(m-1)} \tag{18}$$

From the beam-column deformation diagram of the story repetitive element (Fig. 6), it was observed that the relative displacement between floors under the load generated the included angle, γ, between the string line and plumb line after the frame underwent deformation. Based on the geometric relationship after deformation, the included angle, γ, can be obtained using Eq. (19).

$$\gamma = \frac{\delta}{h} = \frac{(2m-3)h^2}{24EI_c(m-1)^2} + \frac{hl}{12EI_b(m-1)} \tag{19}$$

Because the shear force of the floor is equal to the product of the lateral stiffness of the floor and the lateral displacement of the floor, that is, $V = K\delta$, and $V = GA\cdot\gamma$, Accordingly, the lateral stiffness of the floor can be determined accordingly from Eq. (19).

$$k = \frac{24EI_c(m-1)^2/h^3}{2m-3+\frac{2I_c(m-1)}{I_b}\frac{l}{h}} \tag{20}$$

As the frame bottom is constrained to the fixed end, it is assumed that the antibending point of the column is 2/3 of the story height. Based on the above figure multiplication, the approximate calculation formula for obtaining the lateral stiffness of the bottom floor is derived as follows:

$$k = \frac{18EI_c(m-1)^2/h^3}{(2m-3)+\frac{I_c(m-1)}{3I_b}\cdot\frac{l}{h}} \tag{21}$$

3.2 Calculation Formula for Overall Lateral Stiffness of Flexural-Type Braced Frame Structure

After superimposing the lateral stiffness and bracing stiffness of each floor, the stiffness parameters were substituted into Eq. (17). The formula for calculating the overall lateral stiffness of flexural-type braced frame structures is derived as follows:

$$\begin{aligned}\frac{1}{K_i} = &\frac{1}{\frac{18EI_{c1}(m_1-1)^2/h_1^3}{(2m_1-3)+\frac{I_{c1}(m_1-1)}{3I_{b1}(2m_1+1)}\cdot\frac{l_1}{h_1}}+c_{w1}} + \\ &+\frac{1}{\frac{24EI_{c2}(m_2-1)^2/h_2^3}{(2m_2-3)+\frac{2I_{c2}(m_2-1)}{I_{b2}}\cdot\frac{l_2}{h_2}}+c_{w2}}+\ldots+ \\ &+\frac{1}{\frac{24EI_{ci}(m_i-1)^2/h_i^3}{(2m_i-3)+\frac{2I_{ci}(m_i-1)}{I_{bi}}\cdot\frac{l_i}{h_i}}+c_{wi}}\end{aligned} \tag{22}$$

where m_i is the total number of frame columns on the i^{th} floor. If the inertial moments of the beam and column of the story repetitive element are not equal and the beam-column linear stiffness ratio is $0.3 \le hI_b / (lI_c) \le 5$, the average inertia moment of the beam and column can be obtained. If the beams do not have the same length and the adjacent span difference does not exceed three, the average span can be used. $c_{w1}, c_{w2}, \cdots, c_{wn}$ is the bracing stiffness of each floor provided by the flexural-type braced structure. The bracing structure can be considered a flexural-type cantilever beam. When the stiffness of the bracing structure remains unchanged, computations can be performed using Eq. (23a):

$$c_{wi} = \frac{3EI_w}{H_i^3} \tag{23a}$$

where EI_w is the bending stiffness of the bracing structure and H_i is the total height of the i^{th} floor, as shown in Fig. 4. In an actual building, stiffness often varies with the height of the building. Assuming that the stiffness varies linearly in the height direction, bracing stiffness c_{wi} provided by the bracing structure for the frame is integrated in the direction of the building height. Eq. (23a) can then be rewritten as follows:

$$c_{wi} = EI_{w1} / \int_0^{H_i} \frac{(H_i - x)^2}{1 - x(1 - I_{wi} / I_{w1}) / H_i} \mathrm{d}_x \tag{23b}$$

4 CALCULATION FORMULA OF OVERALL STABILITY OF FLEXURAL-TYPE BRACED FRAME STRUCTURES

Under a vertical load, the column becomes unstable when the critical load is reached, and the load stiffness decreases the lateral stiffness of the column to zero. From Eq. (3), the critical balance equation for any separated column of the flexural-type braced frame structure is expressed as follows:

$$k_{ij} - \alpha_{ij} \frac{N_{ij}}{h_i} = 0 \tag{24}$$

where N_{ij} is the axial force of the j^{th} column on the i^{th} floor and h_i is the height of the i^{th} floor.

In the critical state, the overall lateral stiffness of the flexural-typed braced frame structure is reduced to zero by the load stiffness, therefore, it is $K_i - K_{pi} = 0$. The load stiffness of each floor was assembled using the method for analyzing the overall lateral stiffness of the structure expressed by Eq. (17) to derive Eq. (25).

$$\frac{1}{K_{Pi}} = \frac{1}{k_{P1}} + \frac{1}{k_{P2}} + \ldots + \frac{1}{k_{Pi}} \tag{25}$$

where K_{Pi} is the overall load stiffness of the i^{th} floor of flexural-type braced frame structure. $k_{p1}, k_{p2}, \ldots, k_{pi}$ are the load stiffness parameters of each floor of the flexural-type braced frame structure. Eq. (24) is transformed to derive Eq. (26).

$$k_{Pi} = \lambda_i \sum_{j=1}^{m} \frac{\alpha_{ij} N_{ij}}{h_i} = \lambda_i N_{\min} \sum_{j=1}^{m} \frac{\alpha_{ij} \xi_{ij}}{h_i} \tag{26}$$

In Eq. (26), λ_i is the critical factor of the i^{th} floor. It was assumed that the axial force of each column acted proportionally, and the minimum axial force of the column, $N_{\min}$, was selected as the common factor for calculations. That is, $N_{ij} = \xi_{ij} N_{\min}$, where ξ_{ij} is the proportionality coefficient.

Eq. (26) is substituted into Eq. (25) to obtain the overall load stiffness of each floor:

$$\frac{1}{K_{Pi}} = \frac{1}{\lambda_i N_{\min}} \left(\frac{1}{\sum_{j=1}^{m} \frac{\alpha_{1j} \xi_{1j}}{h_1}} + \frac{1}{\sum_{j=1}^{m} \frac{\alpha_{2j} \xi_{2j}}{h_2}} + \ldots + \frac{1}{\sum_{j=1}^{m} \frac{\alpha_{ij} \xi_{ij}}{h_i}} \right) \tag{27}$$

The principle in which the overall lateral stiffness of the structure is decreased to zero by the load stiffness during instability was applied. Thus, $K_i = K_{Pi}$, that is, $\frac{1}{K_i} = \frac{1}{K_{Pi}}$. The critical force equation of the flexural-type braced frame structure is derived from Eqs. (17) and (27), as follows:

$$\begin{aligned} &\frac{1}{k_1} + \frac{1}{k_2} + \ldots + \frac{1}{k_i} = \\ &= \frac{1}{\lambda_i N_{\min}} \left(\frac{1}{\sum_{j=1}^{m} \frac{\alpha_{1j} \xi_{1j}}{h_1}} + \frac{1}{\sum_{j=1}^{m} \frac{\alpha_{2j} \xi_{2j}}{h_2}} + \ldots + \frac{1}{\sum_{j=1}^{m} \frac{\alpha_{ij} \xi_{ij}}{h_i}} \right) \end{aligned} \tag{28}$$

The critical force of a flexural-type braced frame structure can be calculated using Eq. (28). However, this formula expresses the premise condition of simultaneous instability of each floor; that is, the critical factor λ_i of each floor is equal. In practical applications, instability of each floor without a mutual brace is rare. If Eq. (28) is used to calculate the overall stability of flexural-type braced frame structures, a significant deviation occurs. Therefore, it is necessary to analyze the interactions between different floors. The floor critical factor, λ_i, is calculated using the floor axial force root-mean-square averaged method to reflect the interactions. The revised formula for determining the critical force of flexural-type braced frame structures is expressed as follows:

$$\lambda = \sqrt{\left(N_1 \eta \lambda_1^2 + \sum_{i=2}^{n} N_2 \lambda_i^2 \right) \Big/ \left(N_1 \eta + \sum_{i=2}^{n} N_i \right)} \tag{29a}$$

$$(N_{ij})_{\mathrm{cr}} = \xi_{ij} (\lambda N_{\min}) \tag{29b}$$

where $N_1, N_2, \cdots, N_n$ is the sum of axial forces of each floor, and $\lambda_1, \lambda_2, \cdots, \lambda_n$ is the critical factor of each floor of the flexural-type braced frame structures, which can be

determined using Eq. (28). $(N_{ij})_{cr}$ is the critical force of the j^{th} column on the i^{th} floor; η is the correction coefficient of the weight of the bottom axial force, which reflects the constraint effect of the fixed end at the bottom floor.

$$\eta = \frac{1}{n\chi} \tag{30a}$$

$$\chi = \begin{cases} \frac{c_{w1}}{c_{wT1}} \text{.....when } c_{w1} \geq c_{wT1} \\ \frac{c_{wT1}}{c_{w1}} \text{.....when } c_{w1} \prec c_{wT1} \end{cases} \tag{30b}$$

In Eq. (30), c_{wT1} is the sum of the critical lateral stiffness of each column at the bottom floor, and it is determined using Eq. (10).

When the critical force of each column is determined, Eq. (31) can be used to compute the effective length coefficient of each column to verify the column design of the flexural-type braced frame structure.

$$\mu_{ij} = \sqrt{\frac{\pi^2 EI_{ij}}{(N_{ij})_{cr} h_i^2}} \tag{31}$$

In Eq. (31), I_{ij} is the inertia moment of the j^{th} column on the i^{th} floor.

5 EXAMPLE

A public building with 12 floors was selected as a representative flexural-type braced frame structure (Fig. 8). The bracing structure was a shear wall. The section height of the shear wall was 250 cm, and the thickness gradually changed with the building height: 30 cm (Floors 1 to 4), 25 cm (Floors 5 to 8), and 20 cm (Floors 9 to 12). The frame column selection was 50 × 50 cm, the beam section was 30 × 75 cm, the height (h) was 400 cm, the elastic modulus was E = 2000 kN/cm^2, and the load was P = 2500 kN. The method described in this paper was used to determine the overall stability of the structure and the effective length coefficient of diagram column on each floor.

The steps in solving the problem are as follows.

(1) The thickness of the shear wall gradually changed with increasing height. The bracing stiffness of each floor was determined using Eq. (23), and the lateral stiffness of each floor of the structure was obtained using Eq. (22). The detailed results are presented in Tab.1.

(2) The critical lateral stiffness of the bottom floor obtained using Eq. (10) was compared with the bracing stiffness of the bottom floor. The second-order effect coefficient, α_{ij}, of each column was obtained using Eqs. (14) and (16), as shown in Fig. 8. The load acting on the shear wall was distributed to each frame column based on the load ratio of each column on the same floor. The load stiffness, k_{Pi}, of each floor was computed using Eq. (26). The detailed results are also presented in Tab. 1.

(3) The overall lateral stiffness, K_i, and overall load stiffness, k_{Pi}, of each floor of the structure were determined using Eqs. (22) and (27), respectively. The critical factor, λ_i, of each floor and the overall critical factor, λ, of the structure were obtained using Eqs. (28) and (29a), respectively. The detailed results are presented in Tab. 1.

(4) The critical force $(N_{ij})_{cr}$ of each column was determined using Eq. (29b), and the effective length coefficient, μ_{ij}, of each column of the structure was computed using Eq. (31). The detailed results are presented in Tab. 1.

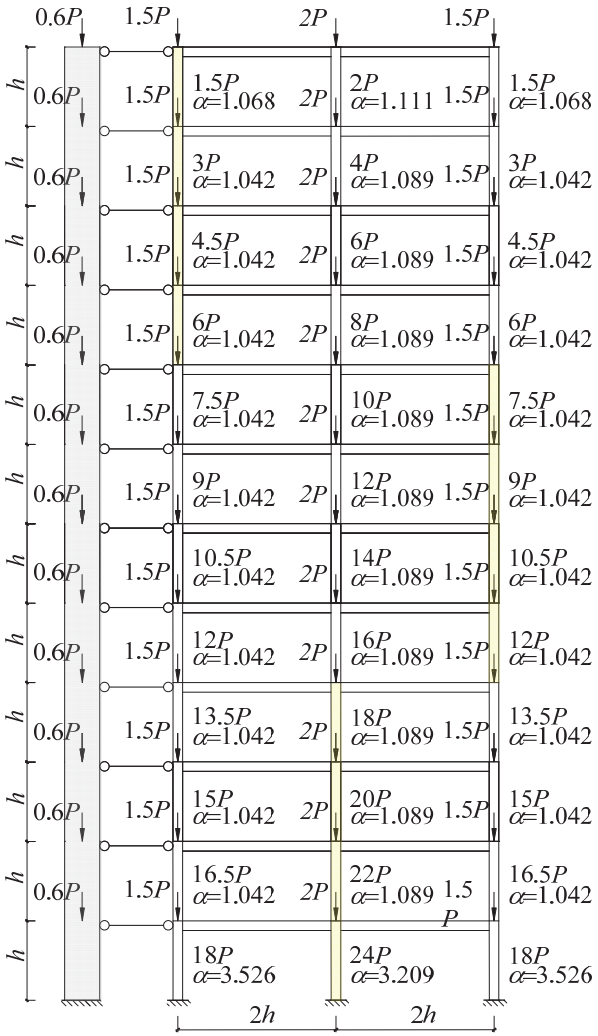

Figure 8 12-layer-frame-core wall structure

The finite element software, ANSYS, was used for computations. In the ANSYS solution, the shell 43 element was used for the shear wall, and the beam 3 element was used for the beams and columns. The joints were rigidly connected for elastic buckling analysis, in which the effects of shear and axial deformations were ignored.

The comparison error between the results obtained using the proposed method and ANSYS is within 2% (Tab. 1). Thus, the calculation accuracy is excellent, indicating that the effect of the brace acting on the frame, the mutual support of columns on the same floor, and the interactions between different floors were fully considered.

In this example, the minimum value of the critical factor is 0.991 for the sixth floor, suggesting that this floor is weak. The overall critical factor, λ, of the structure is 1.289, indicating that this floor receives support from

floors with higher stiffness values. The critical force on this floor increased by 30%. The critical factors of Floors 4 to 10 are lower than the overall critical factor of the structure, indicating that these floors do not have sufficient stiffness but receive support from other floors with higher stiffness. The critical factors of the first, second, 11th, and 12th floors are higher than the overall critical factor of the structure, demonstrating that these floors have high stiffness and can provide stiffness support for floors with lower stiffness values, and the critical force decreases slightly. The first floor had the maximum critical factor (2.772), and its degree of stiffness support was the highest, mainly because of the most significant bracing effect of the shear wall acting on the bottom floor of the frame. The critical factor of the 12th floor was 1.924 (Tab. 1), mainly attributed to the small axial force acting on this floor and the low degree of load stiffness.

Table 1 Compare results of the critical force and the effective length coefficient

Floor	Lateral stiffness provided by columns $\sum k_{ij}$	Bracing stiffness c_{wi}	Lateral stiffness of each floor k_i	Load stiffness of each floor k_{Pi}	The overall lateral stiffness K_i	The overall load stiffness K_{Pi}	Critical factor of each floor λ_i	The overall critical factor λ	$(N_{ij})_{cr}$ ①	ANAYS ②	①/②	μ_{ij} ③	ANAYS ④	③/④
12	224.780	1.933	226.713	37.982	23.630	12.280	1.924		4834	4784	1.010	3.646	3.665	0.995
11	224.780	2.531	227.311	74.256	26.379	18.148	1.454		9668	9567	1.011	2.578	2.592	0.995
10	224.780	3.397	228.177	111.384	29.842	24.017	1.243		14501	14351	1.010	2.105	2.116	0.995
9	224.780	4.696	229.476	148.512	34.332	30.620	1.121		19335	19134	1.011	1.823	1.833	0.995
8	224.780	6.741	231.521	185.640	40.371	38.573	1.047		24169	23918	1.010	1.631	1.639	0.995
7	224.780	10.142	234.922	222.768	48.897	48.689	1.004		29003	28701	1.011	1.488	1.496	0.995
6	224.780	16.232	241.012	259.896	61.748	62.307	**0.991**	**1.289**	33836	33485	1.010	1.378	1.385	0.995
5	224.780	28.256	253.036	297.024	83.015	81.956	1.013		38670	38268	1.011	1.289	1.296	0.995
4	224.780	55.605	280.385	334.152	123.544	113.186	1.092		58005	57402	1.011	1.053	1.058	0.995
3	224.780	132.78	357.560	371.280	220.847	171.164	1.290		64450	63780	1.011	0.998	1.004	0.995
2	224.780	451.43	676.210	408.408	577.544	317.564	1.819		70895	70158	1.011	0.952	0.957	0.995
1	320.318	3637.1	3957.42	1427.66	3957.42	1427.66	2.772		77340	76536	1.011	0.911	0.916	0.995

6 CONCLUSION

1) The calculation formula for the overall stability of flexural-type braced frame structures derived in this study reflects the effect of the brace acting on the frame, the mutual support of columns on the same floor, and the interactions between different floors. Thus, an analytical verification method was developed to verify the accuracy and reliability of the overall stability calculation results of the finite element.

2) A method was established to quantitatively calculate the degree of support between different floors of the flexural-type braced frame structures. This method identifies the location of weak floors and quantitatively analyzes the degree of improvement in the critical force of the floor. The method is suitable for both steel structures and concrete structures.

Acknowledgments

This work was financially supported by the youth project of joint special fund for local universities in Yunnan province of China (202101BA070001-003), and the National Natural Science Foundation of China (51868034).

7 REFERENCES

[1] GB50017 (2018). *Standard for design of steel structures*. Beijing: China Architecture & Building Press.

[2] ANSI/AISC 360-16 (2016). *Specification for Structural Steel Structures*. Chicago: American Institute of Steel Construction.

[3] EN1993 Eurocode3 (2005). *Design of steel structures*. Brussels: European Committee for Standardization.

[4] Timoshenko, S. P. & Guelleh, J. M. (1956). *The Theory of elastic stability, 2nd ed*. Beijing: Science Press.

[5] Aristizabal-Ochoa, J. D. (1997). Stability and minimum bracing for stepped columns with semirigid connections: classical elastic approach. *Structural Engineering & Mechanics*, *5*(4), 415-431. https://doi.org/10.12989/sem.1997.5.4.415

[6] Chen, S. F. (2005). *Guide to stability design of steel structures*. Beijing: China Architecture & Building Press.

[7] Mageirou, G. E. & Gantes, C. J. (2006). Buckling strength of multi-story sway, non-sway and partially-sway frames with semi-rigid connections. *Journal of Constructional Steel Research*, *62*(9), 893-905. https://doi.org/10.1016/j.jcsr.2005.11.019

[8] Rosman, R. (1974). Stability and dynamics of shear-wall frame structures. *Building Science*, *9*(1),55-63. https://doi.org/10.1016/0007-3628(74)90040-1

[9] Bozdogan, K. B. & Ozturk, D. (2010). An approximate method for lateral stability analysis of wall-frame buildings including shear deformations of walls. *Sadhana*, *35*(3), 241-253. https://doi.org/10.1007/s12046-010-0008-y

[10] Hellesland, J. (2009). Extended second order approximate analysis of frames with sway braced column interaction. *Journal of Constructional Steel Research*, *65* (5),1075-1086. https://doi.org/10.1016/j.jcsr.2008.08.008

[11] Saffari, H. & Yazdi, H. M. (2010). An efficient and direct method for out-of-plane buckling analysis of Y-braced steel frames. *Journal of Constructional Steel Research*, *66*(8),

1107-1111. https://doi.org/10.1016/j.jcsr.2010.03.012
[12] Ma, T. & Xu, L. (2020). Shear deformation effects on stability of unbraced steel frames in variable loading. *Journal of Constructional Steel Research*, *164*(Jan). https://doi.org/10.1016/j.jcsr.2019.105811
[13] Ma, T., Zhang, L., & Xu, L. (2021). Effects of beam axial deformations on story-based critical gravity loads in tension-only semi-braced steel frames. *Engineering Structures*, *232*(2). https://doi.org/10.1016/j.engstruct.2021.111862
[14] Tong, G. S. (2004). *In-plane stability of steel structures*. Beijing: China Architecture & Building Press, 146-188.
[15] Rolf, K. (2008). *Stahlbau, Teil 2: Stabilität und theorie ll. Ordnung*. Berlin: Verlag Ernst & Sohn.
[16] Geng, X. Y. & Zhou, D. H. (2014). Universal charts for determining the effective length of compression columns. *Engineering Mechanics*, *31*(8),154-160. https://doi.org/10.6052/j.issn.1000-4750.2013.03.0187
[17] Shuang, C., Zhou, D. H., & Lan S. W. (2019). Simple calculation of critical bearing capacity of sway frame. *Journal of Huazhong University of Science and Technology (Natural Science Edition)*, *47*(8), 55-59. https://doi.org/10.13245/j.hust.190811
[18] Zeng, X. T. & Fan, Y. J. (2008). *Structural mechanics*. Zhengzhou: Zhengzhou University Press.

Contact information:

Shuwei LAN, PhD
Faculty of Architecture and Civil Engineering, Kunming University,
No.2 Puxin Road, Economic and Technological Development Zone,
Kunming, Yunnan 650214, China
E-mail: lanshuwei2000@163.com

Chi XIAO, PhD
(Corresponding author)
Institute of Mechanics, Chinese Academy of Science,
No. 15 North Fourth Ring West Road, Haidian District,
Beijing 100080, China
E-mail: sdwsxc@126.com

Xu CHEN, Associate Professor, PhD
College of Architecture and Civil Engineering, Kunming University,
No.2 Puxin Road, Economic and Technological Development Zone,
Kunming, Yunnan 650214, China
E-mail: 126958074@qq.com

Chunhua WANG, Professor, MSc
College of Architecture and Civil Engineering, Kunming University,
No.2 Puxin Road, Economic and Technological Development Zone,
Kunming, Yunnan 650214, China
E-mail: 871713997@qq.com